Current Research in Food Science 9 (2024) 100784

Contents lists available at ScienceDirect

Current Research in Food Science

journal homepage: www.sciencedirect.com/journal/current-research-in-food-science

Deep machine learning identified fish flesh using multispectral imaging

Zhuoran Xun [a], Xuemeng Wang [b], Hao Xue [a], Qingzheng Zhang [a], Wanqi Yang [a], Hua Zhang [a], Mingzhu Li [a], Shangang Jia [c,**], Jiangyong Qu [a,***], Xumin Wang [a,*]

[a] College of Life Sciences, Yantai University, Yantai, 264005, China
[b] College of Resources and Environment, University of Chinese Academy of Sciences, Beijing, 100049, China
[c] College of Grassland Science and Technology, China Agricultural University, Beijing, 100193, China

ARTICLE INFO

Keywords:
Convolutional neural network
Feature selection
Fish species identification
Machine learning
Multispectral imaging

ABSTRACT

Food fraud is widespread in the aquatic food market, hence fast and non-destructive methods of identification of fish flesh are needed. In this study, multispectral imaging (MSI) was used to screen flesh slices from 20 edible fish species commonly found in the sea around Yantai, China, by combining identification based on the mitochondrial *COI* gene. We found that nCDA images transformed from MSI data showed significant differences in flesh splices of the 20 fish species. We then employed eight models to compare their prediction performances based on the hold-out method with 70% training and 30% test sets. Convolutional neural network (CNN), quadratic discriminant analysis (QDA), support vector machine (SVM), and linear discriminant analysis (LDA) models perform well on cross-validation and test data. CNN and QDA achieved more than 99% accuracy on the test set. By extracting the CNN features for optimization, a very high degree of separation was obtained for all species. Furthermore, based on the Gini index in RF, 11 bands were selected as key classification features for CNN, and an accuracy of 98% was achieved. Our study developed a successful pipeline for employing machine learning models (especially CNN) on MSI identification of fish flesh, and provided a convenient and non-destructive method to determine the marketing of fish flesh in the future.

1. Introduction

Aquatic foods provide approximately 17% of animal protein and 7% of all protein, and this proportion is higher in some developing countries. In 2020, global aquatic animal production was estimated to be 178 million tons, 89% of which was used for human consumption, with fish accounting for more than 84% of all aquatic animals (FAO, 2022). Increasing awareness and demand for fish, the similarity and diversity of existing seafood species, and stock constraints in the food market have led to the detection of fraud at all levels of the seafood supply chain (Fox et al., 2018; Hassoun et al., 2020; McCallum et al., 2022). Replacing high-value species with inexpensive fish is one of the most common forms of fraud. Food fraud for the purpose of economic interests while making illegal profits also produces food quality and safety issues. For example, fish that are toxic, with high levels of mercury, are mislabeled as pufferfish or swordfish (Lawrence et al., 2022). Especially for fish fillet, the difficulty of human sensory evaluation (HSE) has greatly increased due to the loss of the overall appearance of fish. The best response to food fraud is the use of available methods to detect food quality.

Many species identification methods have been developed for use in supply chains to address fraudulent behavior. Solutions based on nucleic acid molecular analyses, such as DNA barcoding and real-time PCR analysis, are widely used (Cardeñosa et al., 2019). The FASTFISH-ID platform is based on nucleic acid sequences for species identification (Naaum et al., 2021). Mass spectrometry combined with chemical analyses (Gatmaitan et al., 2021), proteomics (Gu et al., 2020), and lipidomics (Song et al., 2020) are alternative methods. Although these techniques have proven their accuracy and sensitivity, they require multiple instruments and professionals to process the samples and analyze the results, all of which are time-consuming and require chemical treatment of the samples. Therefore, rapid, nondestructive testing is required for the routine examination of fish flesh.

Spectroscopy combined with machine learning is considered one of

* Corresponding author.
** Corresponding author.
*** Corresponding author.
E-mail addresses: shangang.jia@cau.edu.cn (S. Jia), qjy@ytu.edu.cn (J. Qu), wangxm@ytu.edu.cn (X. Wang).

https://doi.org/10.1016/j.crfs.2024.100784
Received 18 April 2024; Received in revised form 3 June 2024; Accepted 13 June 2024
Available online 14 June 2024
2665-9271/© 2024 The Authors. Published by Elsevier B.V. This is an open access article under the CC BY-NC-ND license (http://creativecommons.org/licenses/by-nc-nd/4.0/).

the most promising nondestructive testing techniques for distinguishing fish flesh. Machine learning makes predictions by learning from examples (training data) to obtain reasonable approximations without an explicit solution algorithm (Deng et al., 2021). The spectral reflection of flesh depends on the movement of molecules and atoms or changes in atomic energy levels to form a detailed fingerprint (Khaled et al., 2021). Spectral technology is often applied in food inspection, including flesh freshness (Robert et al., 2021b; Shin et al., 2021) and species identification (Edwards et al., 2020). Infrared (IR) spectroscopy, Raman spectroscopy, and laser-induced breakdown spectroscopy (LIBS) have proven their reliability in species identification (Kumar and Chandrakant Karne, 2017); for example, the identification of beef, venison, and mutton based on Raman spectra (Robert et al., 2021a) and the identification of pork, beef and chicken based on LIBS (Bilge et al., 2016). Hyperspectral imaging technology (HSI) has been developed and widely applied in the fields of agriculture and food industry, including fecal matter, microbiological contamination, product quality, physical defects, and food fraud (Falkovskaya and Gowen, 2020). HSI has been used to identify lamb, beef, and pork flesh (Al-Sarayreh et al., 2020) based on the substantial spectral characteristics of objects, but the data acquisition of HSI is time-consuming and redundant. Moreover, owing to spectral data redundancy, data processing is complicated.

Multispectral imaging (MSI) integrates the optimized subsets of HSI, and is therefore more efficient (Wang et al., 2021), while data reduction enables faster in data analysis (Fan and Su, 2022; Khaled et al., 2021). The MSI on the platform of VideometerLab4 contains spectral and spatial information, and each pixel contains spectral information in 19 bands. Spectral data in different regions can be obtained via image segmentation to easily expand the dataset. MSI has been successfully applied to the detection of food freshness (Omwange et al., 2021; Ropodi et al., 2018), microbial quantity assessment (Govari et al., 2021), fish quality grading (Jayasundara et al., 2020), quantification of specific ingredients in flesh (Ma et al., 2015) and classification of beef slices (Li et al., 2021a). However, some studies have also shown that MSI has a relatively poor performance of quality assessment in fish microbial growth (Govari et al., 2021). MSI is rarely used for the identification of fish flesh, although a few studies have reported the rapid identification of fish using LIBS and Raman spectroscopy (Ren et al., 2023) and MSI has also been used for fish identification through the body of the fish (Monteiro et al., 2023).

This study aimed to assess the potential of MSI as a method for rapid species identification in fish flesh. Based on the flesh of 20 fish species and 19 wavelengths in VideometerLab4, models of Random Forest (RF), linear discriminant analysis (LDA), support vector machine (SVM), quadratic discriminant analysis (QDA), and convolutional neural network (CNN), EXtreme gradient boosting (XGBoost), categorical boosting (CatBoost), and light gradient boosting machine (LightGBM) were employed and compared for their performances in fish flesh prediction. DNA barcoding based on COI for data labeling was employed to validate the prediction results. We successfully developed a pipeline to identify various species of fish flesh in a non-destructive and high-throughput way.

2. Materials and methods

2.1. Sampling of fish flesh

A total of 57 fresh fish were collected from local fish markets in Yantai, China, in October and November 2021. The skin near the fish spine was removed with a scalpel, and 4–5 pieces of flesh from each fish were placed in 50 mL centrifuge tubes. One piece was used for species determination using the mitochondrial gene *COI*, and the other pieces were used for prediction based on MSI acquisition. Samples were stored at −20 °C, before being sent to China Agricultural University for multispectral photography in VideometerLab4.

2.2. Species identification using the mitochondrial gene COI

The mitochondrial gene *COI* was used to determine the species based on sequence similarity, and to confirm the prediction of machine learning based on MSI data. DNA was extracted using the TIANamp Marine Animals DNA Kit (TIANGEN BIOTECH, Beijing). PCR amplification was conducted using the extracted DNA as the template, with a reaction mixture volume of 25 μL, consisting of 0.5 μL of DNA, 1 μL each of forward and reverse primers (10 μmol/L), 12.5 μL of 2x Taq Plus Master Mix, and 10 μL of ddH_2O. The primers used for PCR were universal for the fish *COI* gene as follows (Lakra et al., 2011): F1-5′TCAACCAACCACAAAGACATTGGCA3′ and R1-5′ TAGACTTCTGG GTGGCCAAAGAATCA3’. And the PCR cycling conditions were as follows: initial denaturation at 94 °C for 2 min; followed by 30 cycles of 94 °C for 30 s for denaturation; 55 °C for 30 s for annealing; 72 °C for 30 s for extension; and a final extension at 72 °C for 2 min. The PCR products were verified on a 1% agarose gel and sent for sequencing. The sequenced reads were blasted against the NT database on the NCBI website, and the species names were obtained.

2.3. Multispectral image acquisition and data extraction

The multispectral imaging data of fish slices was recorded in a VideometerLab4 (Videometer A/S, Herlev, Denmark), which contained 19 monochrome light-emitting diodes (LEDs). The reflectance of 19 discontinuous bands from ultraviolet A to near infrared ray was collected, i.e., 365, 405, 430, 450, 470, 490, 515, 540, 570, 590, 630, 645, 660, 690, 780, 850, 880, 940, and 970 nm (Wang et al., 2021).

Before collecting the spectral data, water was removed from the surface of the fish flesh in a Petri dish with paper towels. After MSI data recording was conducted, VideometerLab software is used to import the multispectral image files and following processing. The background was removed, and individual fish image was segmented before exporting RGB images (Fig. 1 and Fig. S1A). We split the MSI images into small images of 52*52 pixels and finally obtained 8988 spectral images. Among them, 8588 spectral images were used as training and testing data for the modeling (Fig. S1B). The datasets were divided into 70% training set and 30% test set. For each species, 20 MSI images were used for the final validation. It takes approximately 30 s to take a multispectral operation that captures 19 images corresponding to 19 bands.

2.4. Classification models

In this study, a multispectral differential analysis was first undertaken, involving the evaluation of mean spectral reflectance and the execution of multiple comparisons grounded in Scheffe’s test, specifically at wavelengths of 365 nm and 970 nm. Subsequently, normalized canonical discriminant analysis (nCDA) integrated in VideometerLab was used for binary classification (Wang et al., 2023). nCDA is a supervised Fisher linear classifier based on MSI transformation of the images, and nCDA binary analysis was conducted using VideometerLab software. Thereafter, the generalization abilities of SVM, RF, LDA, QDA, CNN, XGBoost, CatBoost, and LightGBM were compared with the training and test data. Some models require parameter adjustment by grid search. However, after grid search, we found that it could not detect the overfitting problem during parameter adjustment, so we artificially constrain the range of certain parameters to eliminate overfitting as much as possible (Table S1).

RF, CatBoost, LightGBM and XGBoost algorithms are all predictive models based on decision trees. But they belong to different integrated learning methods. The RF algorithm by assembling multiple decision trees, each trained on random subsets of data samples and features. Predictions are made by averaging the vote outcomes from these trees. This approach concurrently provides multi-variable feature importance scoring with low computational expense. A key evaluation metric employed is the mean decrease Gini, it assesses the importance of

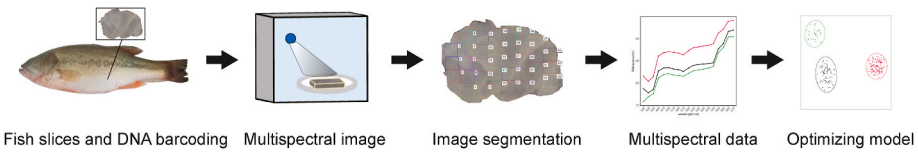

Fig. 1. Flow chart of fish prediction model based on flesh slices and MSI.

variables by calculating the effect of each variable on the heterogeneity of the observations at every node of a classification tree. CatBoost, LightGBM, and XGBoost are all gradient boosting decision tree (GBDT) algorithms, with CatBoost enhancing handling of categorical features and missing values. LightGBM focuses on reducing computational and memory demands, whereas XGBoost optimizes computational efficiency, supports parallel computing, and incorporates regularization into its objective function to control model complexity and overfitting.

SVM are widely-used machine learning techniques that map original data points into a high-dimensional feature space through a kernel function, creating a maximum-margin separating hyperplane with minimal distance to all data points.

LDA is an extension of Fisher's linear discriminant, functioning both as a supervised dimensionality reduction technique and a classification method. LDA aims to maximize between-class variance while minimizing within-class variance. QDA, a variant of LDA, separates classes non-linearly by estimating individual covariance matrices for each class, distinguishing itself as a non-linear classifier but lacking the dimensionality reduction capability of LDA.

The CNN is a promising deep learning method that has been used to analyze various spectral data. In this study, the CNN was used a sequential model from the Keras library (Table 1). The hidden layer consists of four convolutional layer (Conv) and one full connection layer (FC), in which "relu" is used as the activation function for all convolutional layers, and "softmax" is used as the activation function for the FC layer. Conv1 represents the initial convolutional layer with 64 filters of size 1×7. Conv2 comprises three convolution and pooling layers: two maximum pooling layers and one global average pooling layer. Dropout (0.5) refers to the random dropping of 50% of the neurons in the previous layer during training. Using the CNN model above, we added the groups parameter to implement deep convolution (groups = 64) and set the kernel_size and groups parameters to implement point convolution (kernel_size = 1, groups = 1). Combining deep convolution and point convolution forms the convolution operation of DS-CNN. The CNN was run for the training data with the parameters of "optimizer = 'adam', loss = 'sparse_categorical_crossentropy', metrics = 'acc', epochs = 1000, and batch_size = 64". Running of all the models was performed using an AMD Ryzen 5–5600 processor with 6 cores at 3.3 GHz and 16 GB of RAM.

Table 1
The internal structure of CNN model.

	CNN architecture
Conv1	Layers.Conv1D (64, kernel_size = 7, activation = 'relu', padding = 'same')
Conv2	Layers.Conv1D (64, kernel_size = 7, activation = 'relu', padding = 'same') Layers.MaxPooling1D (pool_size = 3) Layers.Conv1D (64, kernel_size = 7, activation = 'relu', padding = 'same') Layers.MaxPooling1D (pool_size = 3) Layers.Dropout (0.5) Layers.Conv1D (64, kernel_size = 7, activation = 'relu', padding = 'same') Layers.GlobalAveragePooling1D
FC	Layers.Dense (20,activation = 'softmax')
output	output categories
Total params	88020

2.5. Model evaluation scheme

The optimal model parameters were selected using a grid search and 10-fold cross-validation, and then the overfitting is adjusted manually. Accuracy (1) represents the overall accuracy of the classification. The precision (2) value is the correctly classified samples divided by all correct samples in a model. The recall (3) value is the correctly classified sample numbers divided by all the samples by the *COI* gene to measure the fraction of positive samples that are correctly classified. Fβ represents the harmonic mean between recall and precision values, while the F1 (β = 1) score (4) considers both equally important (Hossin and Sulaiman, 2015).

With multi-classification models, the overall evaluation is generally performed using micro- or macro-averaged methods. A macro-averaged evaluation indicates that the same weight of each category, and a micro-averaged evaluation indicates that the same weight of each copy. Owing to the imbalance of the data size in this study (Fig. S1B), we chose macro-averages for evaluation with the same degree of emphasis on different categories (Takahashi et al., 2022), referring to the arithmetic average of each statistical index value for any class (Zhang et al., 2021). Therefore, this study evaluated the model using the Accuracy, Macro-P (Macro-Precision) (5), Macro-R (Macro-Recall) (6), and Macro-F1 (7) using the caret package (v6.0.93) in RStudio. Macro-P, Macro-R, and Macro-F1 represent the average precision, recall, and F1, respectively. The equations used are as follows:

$$Accuracy = \frac{TP + TN}{TP + TN + FP + FN} \tag{1}$$

$$P = Precision = \frac{TP}{TP + FP} \tag{2}$$

$$R = Recall = \frac{TP}{TP + FN} \tag{3}$$

$$F1 = 2\frac{P \bullet R}{P + R} \tag{4}$$

$$Macro - P = \frac{1}{n}\sum_{i=1}^{n} Pi \tag{5}$$

$$Macro - R = \frac{1}{n}\sum_{i=1}^{n} Ri \tag{6}$$

$$Macro - F1 = \frac{1}{n}\sum_{i=1}^{n} F1i \tag{7}$$

Here, TP represents true positive, positive samples successfully predicted; FP represents false positive, negative samples falsely predicted to be positive; TN represents true negative, negative samples successfully predicted to be negative; and FN represents false negative, false prediction of negative samples.

3. Results

3.1. Species determination

The *COI* gene was amplified from fish samples using universal

primers, and sequences of 675-bp PCR products with a total of 278 variation sites were subjected to Blastn against the nucleotide database on the NCBI website to determine species names. It was discovered that most samples could be assigned a unique species name, whereas two sequences matched two species with very close scores, and only the genus could be determined for these four samples, that is, *Cleisthenes pinetorum* vs. *Cleisthenes herzensteini*, and *Takifugu rubripes* vs. *Takifugu pseudommus*. It is believed that *Cleisthenes pinetorum* and *Cleisthenes herzensteini* belong to the same species, and *Takifugu rubripes* and *Takifugu pseudommus* belong to a single species (Park et al., 2020; Song et al., 2001; Vinnikov et al., 2018). The sequence alignment results were all greater than 99%, and the sequences were uploaded to NCBI to obtain the GenBank accession numbers. The fish samples were assigned to 20 species from 17 families and 10 orders (Table S2).

3.2. Spectral differences for fish flesh

Multispectral data from 19 bands showed significant differences among the samples (Fig. S2A), which were useful for fish classification. ONk showed a sharp increase in the average reflectance between 540 nm and 630 nm, which differed significantly from that of the other fish. Furthermore, 365 nm and 970 nm were selected to conduct multiple comparisons of the average reflectance of each species (Fig. S2B, Fig. S2C), which revealed significant differences among the samples ($P < 0.01$). For example, COm, TRIj, and GAm were similar at 365 nm, but differed at 970 nm ($P < 0.01$). In addition, the transformation of nCDA was conducted for pairwise species based on MSI data (Fig. S3), which showed that 20 species had spatial and spectral variations. Therefore, MSI data was potentially sufficient to classify fish flesh samples.

3.3. Stability assessment and classification of multiple classification models

To evaluate the effect and stability of the models, we conducted a 10-fold cross-validation for each model under the optimal parameters. The standard deviations of CatBoost, LightGBM, XGBoost and RF models were bigger (0.0183–0.0256) than those of <0.01 in CNN, SVM, QDA, and LDA (Table S3). The prediction performance of each model was consistent with the cross-validation results of the overall evaluation (Table 2). Among them, the accuracies of CatBoost, LightGBM, XGBoost, and RF models in the overall evaluation were 65.85–77.42%. The overfitting of the RF model could not be corrected by adjusting the parameters. In addition, Macro-R, macro-P, Macro-F1 in these four models were between 0.6125 and 0.7493, indicating poor classification ability for some categories. The accuracies of SVM, QDA, and CNN were greater than 95%, and the scores of Macro-R, Macro-P, and Macro-F1 ranged from 0.95 to 0.99, indicating a good classification ability. QDA achieved the training time in less than 1 s under the default parameters.

As a supervised dimension-reduction method, LDA can be used to visualize classification results. The results of LDA dimensionality reduction showed that ONk was completely isolated from all species, and there was also partially distinguishable from other species, especially LOi, CHs, and TRAj, with a high degree of differentiation (Fig. 2).

Table 2
Comparison of eight classification models.

model	Test data prediction				Model training duration	Training data accuracy
	Accuracy	Macro-R	Macro-P	Macro-F1		
CatBoost	71.44%	0.7043	0.6604	0.6817	83.5s	74.53%
LightGBM	65.85%	0.6401	0.6125	0.626	0.4s	79.49%
XGBoost	68.45%	0.6664	0.6351	0.6504	3.1s	77.96%
CNN	99.61%	0.9947	0.9945	0.9946	505.64 s	99.75%
RF	77.42%	0.7186	0.7493	0.7279	1.714 s	100%
SVM	97.97%	0.9694	0.9749	0.9718	4.3418 s	99.53%
LDA	90.52%	0.9107	0.8854	0.8969	0.2011 s	89.40%
QDA	99.37%	0.9914	0.9925	0.9919	0.6976 s	99.45%

3.4. Test accuracy for individual species

The distribution of test data is shown in Fig. S4. The prediction of ONk in all models was almost the easiest, which is in accordance with the spectral curve of ONk (Fig. S2A). The prediction accuracy of CatBoost, LightGBM, XGBoost, and RF models for each species ranged from 5.4% to 100%, with similar patterns. For example, the classification accuracies of these four models for CHs, CLp, and THm were all poor. In contrast, the classification accuracies for PAa, SCn, and LOi were relatively high (Fig. S5). The classification accuracy of LDA for each species was between 77.4% and 100%, and the accuracy of 12 species was greater than 90%, while the classification of SVM was from 88.5% to 100% (Fig. S6). The prediction performance of QDA was good for all species, and obviously, CNN was with >96% accuracies for all species (Fig. 3).

With the best classification effect and stability, CNN was run with a slightly longer model training time. CNN realizes efficient feature extraction from input data through the collaborative action of its convolutional layers, pooling layers, and activation functions, among others. We extracted the CNN features before being input into the FC layer, with filters = 4, to make use of 4-dimensional data (Table S4). The LDA visualization results showed that 20 species were highly distinguishable in the two-dimensional level (Fig. 4). We confirmed that the CNN model combined with MSI was reliable for species classification.

3.5. Feature selection

To specify the wavelengths sufficient for classification, feature selection was performed for the two best models: QDA and CNN. The traditional ANOVA method was not optimized for effective feature screening; therefore, we chose feature selection in the RF model based on the importance ranking of the Gini index (Fig. 5A). The first 8–12 features were used to train the two models and predict the accuracy of the test set. The results showed that the CNN classification results were better than those of QDA (Fig. 5B). When the number of features was less than eight, the accuracies in both models decreased significantly. With an accuracy threshold of 98%, the first 11 features were selected in the

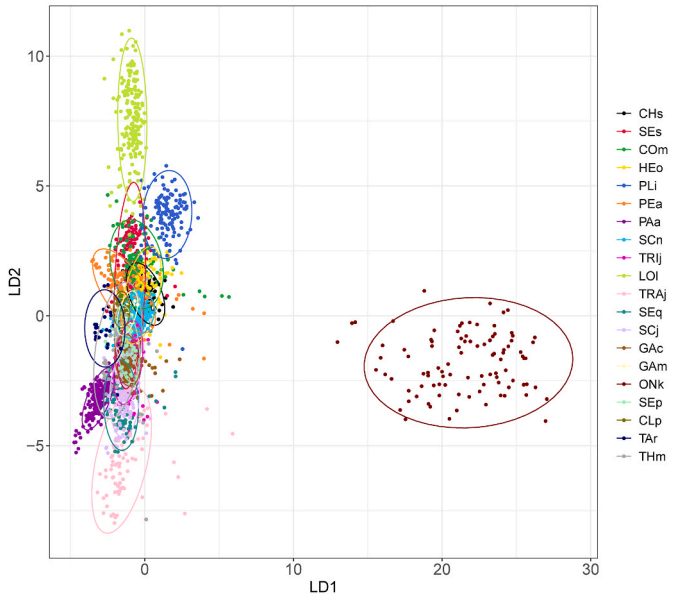

Fig. 2. Visualization of LDA results with LD1 and LD2 dimensions. (Refer to Table S2 for the full names of the fish species.).

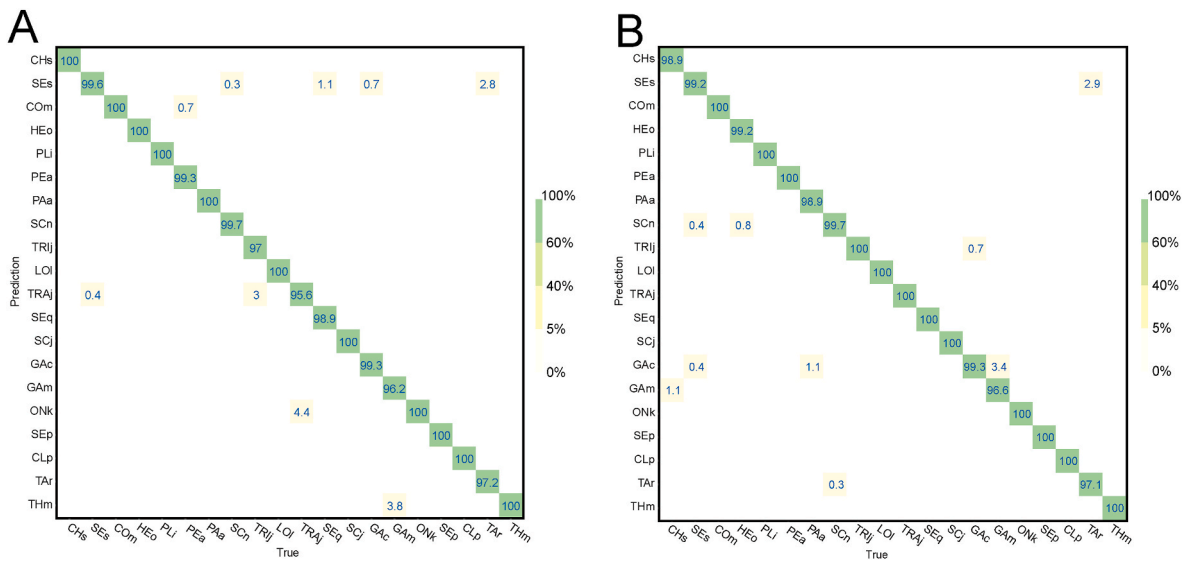

Fig. 3. Prediction accuracy of two models for fish flesh. (A) QDA model confusion matrix; (B) CNN model confusion matrix. (Refer to Table S2 for the full names of the fish species.).

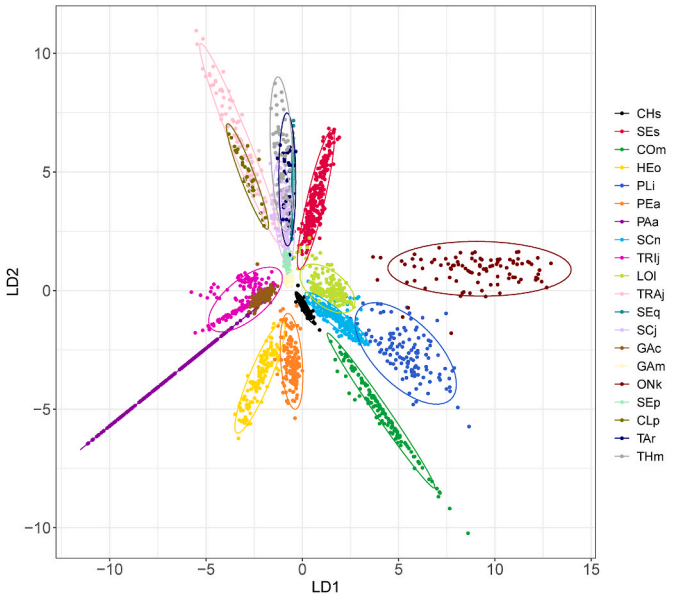

Fig. 4. Visualization of LDA results in LD1 and LD2 dimensions based on CNN extraction features. (Refer to Table S2 for the full names of the fish species.).

CNN. Due to the reduction in features, some parameters of the CNN should be changed to obtain better results. Therefore, the CNN parameters in this section were adjusted with a convolution kernel size (i.e. kernel_size) of 3, a dropout of 0.3, and a training period (i.e., epoch) of 1000. To verify the prediction stability of the model prediction after dimensionality reduction, 400 spectral validation data points not involved in training and testing were used. The results showed that the accuracy reached 99.75%, with only one prediction error.

4. Discussion

The results of this study show that MSI combined with machine learning is an up-and-coming method for fish identification. In addition to DNA barcoding, scientists have developed ways to quickly detect fish by different means, including computer vision based on morphological and textural features of fish (Monteiro et al., 2022; Rauf et al., 2019), DNA extraction and PCR (Kappel et al., 2020; Li et al., 2021b; Naaum et al., 2021); mass spectrometry (De Graeve et al., 2023; Rigano et al., 2019) and spectral fusion (Ren et al., 2023). Disadvantages of these methods included high time-cost, use of organic reagents, and cumbersome data preprocessing (Table S5). Our efforts were in accordance with the previous reports on flesh adulteration and freshness assessment based on MSI and machine learning (Fengou et al., 2021a; Spyrelli et al., 2021, 2022). Research employing MSI combined with machine learning techniques for categorizing sections of fish bodies also demonstrate the investigational potential of MSI (Monteiro et al., 2023). Indeed, there are also studies presenting divergent viewpoints, asserting that Multispectral Imaging (MSI) is less efficacious compared to Fourier Transform Infrared (FT-IR) Spectroscopy in assessing the microbial quality of fish fillets (Govari et al., 2022).

Our data analysis pipeline involved a series of steps, including MSI image segmentation, statistical analysis of spectral data, nCDA binary classification, and up to eight multi-classification models were utilized. Based on identification of 20 fish species, we obtained >95% of classification accuracy for the three models (SVM, QDA, CNN), and even >99% for QDA and CNN. We further narrowed the spectral bands to make a light data analysis with acceptable results. The use of CNN feature extraction reduced the data processing time, and with 11 bands, CNN still can reach 98% accuracy. It represents a new effort to resolve the fast identification of fish flesh in a non-destructive way.

ONK samples with distinct appearance (color) performed best in all models, as the multispectral reflectance peaks at 540 nm and 630 nm matched the absorption peak of astaxanthin at 450–600 nm (Dissing et al., 2011). The 11 key bands selected in this study contain wavelengths of 365, 405, 430, 450, 470, 490, 570, 590, 630, 940 and 970 nm, which showed association with flesh nutrients, including 545, 575, and 635 nm associated with myoglobin and its derivatives (Liu et al., 2003); 880 and 940 nm with fat content, and 970 nm with water content (Sendin et al., 2018; Zhang et al., 2020). Research has indicated that the spectral region for animals muscle identification ranged from 400 nm to at least 970 nm, incorporating wavelengths such as 405, 435, 450, 470, 505, 525, 570, 590, 630, 645, 660, and 970 nm. The absence of wavelengths typically associated with fat content (880 nm, 940 nm), can likely be attributed to the lower fat levels present in the sampled specimens (Fengou et al., 2021b). The multispectral imaging employed in this study did not include wavelengths of >1000 nm in its optimization, such as the 1100–1250 nm, which is fat-related spectral region (Pu et al., 2015). Incorporating such wavelengths might supplement additional

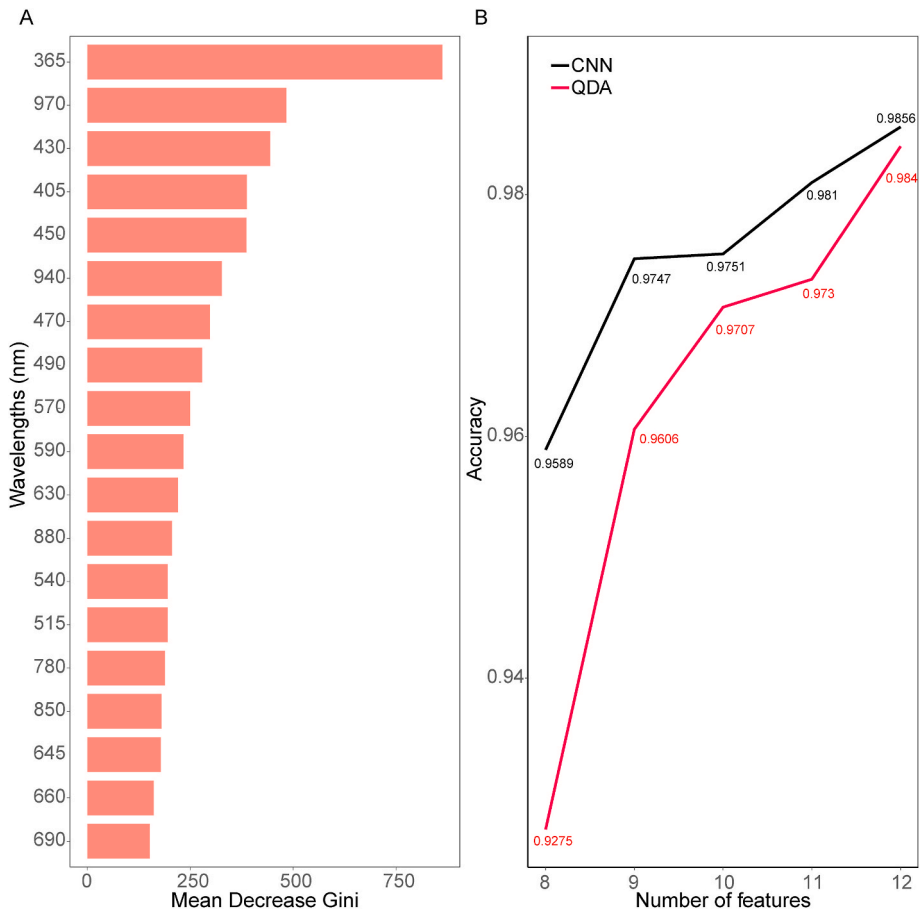

Fig. 5. Feature importance and comparison of QDA and CNN. (A) Feature importance visualization in RF model based on Gini index; (B) Accuracy of CNN and QDA based on features with importance of top ranking 8–12.

information, thereby potentially enhancing the accuracy of fish species identification using multispectral imaging.

The 5-layer CNN model performed the best, probably because it conducts achieve nonlinear classification based on a combination of spectral and spatial data (Kiranyaz et al., 2021; Voigtlaender, 2023). Compared with 2D-CNN, 1D-CNN does not need to transform images, which not only reduces the time of data preprocessing but also greatly reduces the computational complexity (Kiranyaz et al., 2021). Meanwhile, as DS-CNN model is a combination of depth-wise and point-wise convolutions (Shaheed et al., 2022), we tested the performances of DS-CNN (data not shown) on fish flesh in this study. However, it took the training time 4–5 times longer than that by CNN, and it might be due to efficiency of data usage in neural network in terms of time cost on memory access (Ma et al., 2018).

Fish identification method based on MSI established in this study is a fast and non-destructive detection method, and the CNN model has a high prediction accuracy. Our results are of great help for the development of portable identification equipment and the improvement of reporting fraud in the fish market. The scripts have been uploaded into the GitHub website (https://github.com/xunzhuoran/MSI-ML).

Funding

This work was supported by Research and Development Program of Shandong Province, China (Major Science and Technology Innovation Project, Grant No. 2021CXGC011306); the Key Funded with the MNR Key Laboratory of Eco-Environmental Science and Technology, China, MEEST-2021-05; Natural Science Foundation Shandong Province (Grant No. ZR2020MD002); National Key Research and Development Program of China (Grant No. 2021YFC2401005); Research and Development Program of Jilin Province, China (Major Science and Technology Innovation Project, Grant No. 20230304002YY); The Doctoral Science Research Foundation of Yantai University under Grant SM15B01, SM19B70 and SM19B28; Yantai "double-hundred project" (2320004-SM20RC02).

CRediT authorship contribution statement

Zhuoran Xun: Investigation, Data curation, Formal analysis, and interpretation of data, Model construction and, Visualization, Writing – original draft. **Xuemeng Wang:** Acquisition of data, data collation and, Formal analysis. **Hao Xue:** Sample collection, technical support. **Qingzheng Zhang:** Sample collection. **Wanqi Yang:** Sample collection. **Hua Zhang:** Sample collection. **Mingzhu Li:** Sample collection. **Shangang Jia:** Conceptualization, Methodology, Investigation, Writing – review & editing. **Jiangyong Qu:** Project administration, Methodology, Investigation, Funding acquisition. **Xumin Wang:** Project administration, Conceptualization, Methodology, Investigation, Writing – review & editing, All authors approved the version of the manuscript to be published.

Declaration of competing interest

The authors declare that they have no known competing financial interests or personal relationships that could have appeared to influence the work reported in this paper.

Data availability

I have shared the link to my data/code at the Attach File step

Appendix A. Supplementary data

Supplementary data to this article can be found online at https://doi.org/10.1016/j.crfs.2024.100784.

References

Al-Sarayreh, M., Reis, M.M., Yan, W.Q., Klette, R., 2020. Potential of deep learning and snapshot hyperspectral imaging for classification of species in meat. Food Control 117, 107332. https://doi.org/10.1016/j.foodcont.2020.107332.

Bilge, G., Velioglu, H.M., Sezer, B., Eseller, K.E., Boyaci, I.H., 2016. Identification of meat species by using laser-induced breakdown spectroscopy. Meat Sci. 119, 118–122. https://doi.org/10.1016/j.meatsci.2016.04.035.

Cardeñosa, D., Gollock, M.J., Chapman, D.D., 2019. Development and application of a novel real-time polymerase chain reaction assay to detect illegal trade of the European eel (*Anguilla anguilla*). Conservation Science and Practice 1, e39. https://doi.org/10.1111/csp2.39.

De Graeve, M., Birse, N., Hong, Y., Elliott, C.T., Hemeryck, L.Y., V, L., 2023. Multivariate versus machine learning-based classification of rapid evaporative Ionisation mass spectrometry spectra towards industry based large-scale fish speciation. Food Chem. 404, 134632 https://doi.org/10.1016/j.foodchem.2022.134632.

Deng, X., Cao, S., Horn, A.L., 2021. Emerging applications of machine learning in food safety. Annu. Rev. Food Sci. Technol. 12, 513–538. https://doi.org/10.1146/annurev-food-071720-024112.

Dissing, B.S., Nielsen, M.E., Ersboll, B.K., Frosch, S., 2011. Multispectral imaging for determination of astaxanthin concentration in salmonids. PLoS One 6, e19032. https://doi.org/10.1371/journal.pone.0019032.

Edwards, K., Manley, M., Hoffman, L.C., Beganovic, A., Kirchler, C.G., Huck, C.W., Williams, P.J., 2020. Differentiation of South African game meat using Near-Infrared (NIR) spectroscopy and hierarchical modelling. Molecules 25, 1845. https://doi.org/10.3390/molecules25081845.

Falkovskaya, A., Gowen, A., 2020. Literature review: spectral imaging applied to poultry products. Poult Sci 99, 3709–3722. https://doi.org/10.1016/j.psj.2020.04.013.

Fan, K.J., Su, W.H., 2022. Applications of Fluorescence Spectroscopy, RGB- and MultiSpectral imaging for quality determinations of white meat: a Review. Biosensors 12, 76. https://doi.org/10.3390/bios12020076.

FAO, 2022. The State of World Fisheries and Aquaculture 2022. FAO, Rome. https://doi.org/10.4060/cc0461en.

Fengou, A.L., Tsakanikas, P., Mohareb, F., Nychas, G.E., 2021a. Detection of meat adulteration using spectroscopy-based sensors. Foods 10. https://doi.org/10.3390/foods10040861.

Fengou, L.-C., Tsakanikas, P., Nychas, G.-J.E., 2021b. Rapid detection of minced pork and chicken adulteration in fresh, stored and cooked ground meat. Food Control 125, 108002. https://doi.org/10.1016/j.foodcont.2021.108002.

Fox, M., Mitchell, M., Dean, M., Elliott, C., Campbell, K., 2018. The seafood supply chain from a fraudulent perspective. Food Secur. 10, 939–963. https://doi.org/10.1007/s12571-018-0826-z.

Gatmaitan, A.N., Lin, J.Q., Zhang, J., Eberlin, L.S., 2021. Rapid analysis and authentication of meat using the MasSpec Pen Technology. J. Agric. Food Chem. 69, 3527–3536. https://doi.org/10.1021/acs.jafc.0c07830.

Govari, M., Tryfinopoulou, P., Panagou, E.Z., Nychas, G.E., 2022. Application of Fourier transform infrared (FT-IR) spectroscopy, multispectral imaging (MSI) and electronic nose (E-Nose) for the rapid evaluation of the microbiological quality of gilthead sea bream fillets. Foods 11. https://doi.org/10.3390/foods11152356.

Govari, M., Tryfinopoulou, P., Parlapani, F.F., Boziaris, I.S., Panagou, E.Z., Nychas, G.E., 2021. Quest of intelligent research tools for rapid evaluation of fish quality: FTIR spectroscopy and multispectral imaging versus microbiological analysis. Foods 10, 264. https://doi.org/10.3390/foods10020264.

Gu, S., Deng, X., Shi, Y., Cai, Y., Huo, Y., Guo, D., Han, F., 2020. Identification of peptide biomarkers for authentication of Atlantic salmon and rainbow trout with untargeted and targeted proteomics approaches and quantitative detection of adulteration. J Chromatogr B Analyt Technol Biomed Life Sci 1155, 122194. https://doi.org/10.1016/j.jchromb.2020.122194.

Hassoun, A., Mage, I., Schmidt, W.F., Temiz, H.T., Li, L., Kim, H.Y., Nilsen, H., Biancolillo, A., Ait-Kaddour, A., Sikorski, M., Sikorska, E., Grassi, S., Cozzolino, D., 2020. Fraud in animal origin food products: advances in emerging spectroscopic detection methods over the past five years. Foods 9, 1069. https://doi.org/10.3390/foods9081069.

Hossin, M., Sulaiman, M.N., 2015. A review on evaluation metrics for data classification evaluations. International Journal of Data Mining & Knowledge Management Process 5, 1–11.

Jayasundara, D., Ramanayake, L., Senarath, N., Herath, S., Godaliyadda, R., Ekanayake, P., Herath, V., Ariyawansha, S., 2020. Multispectral imaging for automated fish quality grading. Paper Presented at the 2020 IEEE 15th International Conference on Industrial and Information Systems (ICIIS), Rupnagar, India.

Kappel, K., Eschbach, E., Fischer, M., Fritsche, J., 2020. Design of a user-friendly and rapid DNA microarray assay for the authentication of ten important food fish species. Food Chem. 311, 125884 https://doi.org/10.1016/j.foodchem.2019.125884.

Khaled, A.Y., Parrish, C.A., Adedeji, A., 2021. Emerging nondestructive approaches for meat quality and safety evaluation-A review. Compr. Rev. Food Sci. Food Saf. 20, 3438–3463. https://doi.org/10.1111/1541-4337.12781.

Kiranyaz, S., Avci, O., Abdeljaber, O., Ince, T., Gabbouj, M., Inman, D.J., 2021. 1D convolutional neural networks and applications: a survey. Mech. Syst. Signal Process. 151 https://doi.org/10.1016/j.ymssp.2020.107398. Article 107398.

Kumar, Y., Chandrakant Karne, S., 2017. Spectral analysis: a rapid tool for species detection in meat products. Trends Food Sci. Technol. 62, 59–67. https://doi.org/10.1016/j.tifs.2017.02.008.

Lakra, W.S., Verma, M.S., Goswami, M., Lal, K.K., Mohindra, V., Punia, P., Gopalakrishnan, A., Singh, K.V., Ward, R.D., Hebert, P., 2011. DNA barcoding Indian marine fishes. Mol Ecol Resour 11, 60–71. https://doi.org/10.1111/j.1755-0998.2010.02894.x.

Lawrence, S., Elliott, C., Huisman, W., Dean, M., van Ruth, S., 2022. The 11 sins of seafood: assessing a decade of food fraud reports in the global supply chain. Compr. Rev. Food Sci. Food Saf. 21, 3746–3769. https://doi.org/10.1111/1541-4337.12998.

Li, A., Li, C., Gao, M., Yang, S., Liu, R., Chen, W., Xu, K., 2021a. Beef cut classification using multispectral imaging and machine learning method. Front. Nutr. 8, 755007 https://doi.org/10.3389/fnut.2021.755007.

Li, H., Xie, R., Yu, W., Wang, N., Chen, A., 2021b. Rapid identification of cod and oil fish components based on loop-mediated isothermal amplification. Aquaculture 545. https://doi.org/10.1016/j.aquaculture.2021.737209.

Liu, Y., Lyon, B.G., Windham, W.R., Realini, C.E., Pringle, T.D., Duckett, S., 2003. Prediction of color, texture, and sensory characteristics of beef steaks by visible and near infrared reflectance spectroscopy. A feasibility study. Meat Sci. 65, 1107–1115. https://doi.org/10.1016/S0309-1740(02)00328-5.

Ma, F., Qin, H., Zhou, C., Wang, X., Chen, C., Zheng, L., 2015. Rapid and Non-destructive detection of iron porphyrin content in pork using multispectral imaging approach. Food Anal. Methods 9, 1180–1187. https://doi.org/10.1007/s12161-015-0298-0.

Ma, N., Zhang, X., Zheng, H.-T., Sun, J., 2018. ShuffleNet V2: practical guidelines for efficient CNN architecture design. In: Computer Vision – ECCV 2018, pp. 122–138.

McCallum, C.S., Cerroni, S., Derbyshire, D., Hutchinson, W.G., Nayga Jr, R.M., 2022. Consumers' responses to food fraud risks: an economic experiment. Eur. Rev. Agric. Econ. 49, 942–969. https://doi.org/10.1093/erae/jbab029.

Monteiro, F., Bexiga, V., Chaves, P., Godinho, J., Henriques, D., Melo-Pinto, P., Nunes, T., Piedade, F., Pimenta, N., Sustelo, L., Fernandes, A.M., 2023. Classification of fish species using multispectral data from a low-cost camera and machine learning. Rem. Sens. 15 https://doi.org/10.3390/rs15163952.

Monteiro, R.S., Ribeiro, M.C.O., Viana, C.A.S., Moreira, M.W.L., Araúo, G.S., Rodrigues, J.J.P.C., 2022. Fish recognition model for fraud prevention using convolutional neural networks. Advances in Computational Intelligence 3. https://doi.org/10.1007/s43674-022-00048-6.

Naaum, A.M., Cusa, M., Singh, M., Bleicher, Z., Elliott, C., Goodhead, I.B., Hanner, R.H., Helyar, S.J., Mariani, S., Rice, J.E., Wangh, L.J., Sanchez, J.A., 2021. Validation of FASTFISH-ID: a new commercial platform for rapid fish species authentication via universal closed-tube barcoding. Food Res. Int. 141, 110035 https://doi.org/10.1016/j.foodres.2020.110035.

Omwange, K.A., Saito, Y., Zichen, H., Khaliduzzaman, A., Kuramoto, M., Ogawa, Y., Kondo, N., Suzuki, T., 2021. Evaluating Japanese dace (*Tribolodon hakonensis*) fish freshness during storage using multispectral images from visible and UV excited fluorescence. Lwt 151, 112207. https://doi.org/10.1016/j.lwt.2021.112207.

Park, Y.J., Lee, M.N., Noh, J.K., Noh, E.S., Kang, J.H., Park, J.Y., Kim, E.M., 2020. Classification of *Takifugu rubripes, T. chinensis* and *T. pseudommus* by genotyping-by-sequencing. PLoS One 15, e0236483. https://doi.org/10.1371/journal.pone.0236483.

Pu, H., Kamruzzaman, M., Sun, D.-W., 2015. Selection of feature wavelengths for developing multispectral imaging systems for quality, safety and authenticity of muscle foods-a review. Trends Food Sci. Technol. 45, 86–104. https://doi.org/10.1016/j.tifs.2015.05.006.

Rauf, H.T., Lali, M.I.U., Zahoor, S., Shah, S.Z.H., Rehman, A.U., Bukhari, S.A.C., 2019. Visual features based automated identification of fish species using deep convolutional neural networks. Comput. Electron. Agric. 167 https://doi.org/10.1016/j.compag.2019.105075.

Ren, L., Tian, Y., Yang, X., Wang, Q., Wang, L., Geng, X., Wang, K., Du, Z., Li, Y., Lin, H., 2023. Rapid identification of fish species by laser-induced breakdown spectroscopy and Raman spectroscopy coupled with machine learning methods. Food Chem. 400, 134043 https://doi.org/10.1016/j.foodchem.2022.134043.

Rigano, F., Mangraviti, D., Stead, S., Martin, N., Petit, D., Dugo, P., Mondello, L., 2019. Rapid evaporative ionization mass spectrometry coupled with an electrosurgical knife for the rapid identification of Mediterranean Sea species. Anal. Bioanal. Chem. 411, 6603–6614. https://doi.org/10.1007/s00216-019-02000-z.

Robert, C., Fraser-Miller, S.J., Jessep, W.T., Bain, W.E., Hicks, T.M., Ward, J.F., Craigie, C.R., Loeffen, M., Gordon, K.C., 2021a. Rapid discrimination of intact beef, venison and lamb meat using Raman spectroscopy. Food Chem. 343, 128441 https://doi.org/10.1016/j.foodchem.2020.128441.

Robert, C., Jessep, W., Sutton, J.J., Hicks, T.M., Loeffen, M., Farouk, M., Ward, J.F., Bain, W.E., Craigie, C.R., Fraser-Miller, S.J., Gordon, K.C., 2021b. Evaluating low-mid- and high-level fusion strategies for combining Raman and infrared spectroscopy for quality assessment of red meat. Food Chem. 361, 130154 https://doi.org/10.1016/j.foodchem.2021.130154.

Ropodi, A.I., Panagou, E.Z., Nychas, G.E., 2018. Rapid detection of frozen-then-thawed minced beef using multispectral imaging and Fourier transform infrared spectroscopy. Meat Sci. 135, 142–147. https://doi.org/10.1016/j.meatsci.2017.09.016.

Sendin, K., Manley, M., Williams, P.J., 2018. Classification of white maize defects with multispectral imaging. Food Chem. 243, 311–318. https://doi.org/10.1016/j.foodchem.2017.09.133.

Shaheed, K., Mao, A., Qureshi, I., Kumar, M., Hussain, S., Ullah, I., Zhang, X., 2022. DS-CNN: a pre-trained Xception model based on depth-wise separable convolutional neural network for finger vein recognition. Expert Syst. Appl. 191 https://doi.org/10.1016/j.eswa.2021.116288.

Shin, S., Lee, Y., Kim, S., Choi, S., Kim, J.G., Lee, K., 2021. Rapid and non-destructive spectroscopic method for classifying beef freshness using a deep spectral network fused with myoglobin information. Food Chem. 352, 129329 https://doi.org/10.1016/j.foodchem.2021.129329.

Song, G., Chen, K., Wang, H., Zhang, M., Yu, X., Wang, J., Shen, Q., 2020. In situ and real-time authentication of Thunnus species by iKnife rapid evaporative ionization mass spectrometry based lipidomics without sample pretreatment. Food Chem. 318, 126504 https://doi.org/10.1016/j.foodchem.2020.126504.

Song, L., Liu, B., Xiang, J., Qian, P.Y., 2001. Molecular phylogeny and species identification of pufferfish of the genus *Takifugu* (Tetraodontiformes, Tetraodontidae). Mar. Biotechnol. 3, 398–406. https://doi.org/10.1007/s10126-001-0006-5.

Spyrelli, E.D., Nychas, G.E., Panagou, E.Z., 2022. Assessment of the microbial spoilage and quality of marinated chicken souvlaki through spectroscopic and biomimetic sensors and data fusion. Microorganisms 10. https://doi.org/10.3390/microorganisms10112251.

Spyrelli, E.D., Papachristou, C.K., Nychas, G.E., Panagou, E.Z., 2021. Microbiological quality assessment of chicken thigh fillets using spectroscopic sensors and multivariate data analysis. Foods 10. https://doi.org/10.3390/foods10112723.

Takahashi, K., Yamamoto, K., Kuchiba, A., Koyama, T., 2022. Confidence interval for micro-averaged F1 and macro-averaged F1 scores. Appl. Intell. 52, 4961–4972. https://doi.org/10.1007/s10489-021-02635-5.

Vinnikov, K.A., Thomson, R.C., Munroe, T.A., 2018. Revised classification of the righteye flounders (Teleostei: pleuronectidae) based on multilocus phylogeny with complete taxon sampling. Mol. Phylogenet. Evol. 125, 147–162. https://doi.org/10.1016/j.ympev.2018.03.014.

Voigtlaender, F., 2023. The universal approximation theorem for complex-valued neural networks. Appl. Comput. Harmon. Anal. 64, 33–61. https://doi.org/10.1016/j.acha.2022.12.002.

Wang, X., Zhang, H., Song, R., He, X., Mao, P., Jia, S., 2021. Non-destructive identification of naturally aged alfalfa seeds via multispectral imaging analysis. Sensors 21, 5804. https://doi.org/10.3390/s21175804.

Wang, X., Zhang, H., Song, R., Sun, M., Liu, P., Tian, P., Mao, P., Jia, S., 2023. Multiple omics datasets reveal significant physical and physiological dormancy in alfalfa hard seeds identified by multispectral imaging analysis. The Crop Journal 11, 1458–1468. https://doi.org/10.1016/j.cj.2023.03.003.

Zhang, H., Zhang, S., Chen, Y., Luo, W., Huang, Y., Tao, D., Zhan, B., Liu, X., 2020. Non-destructive determination of fat and moisture contents in Salmon (*Salmo salar*) fillets using near-infrared hyperspectral imaging coupled with spectral and textural features. J. Food Compos. Anal. 92 https://doi.org/10.1016/j.jfca.2020.103567.

Zhang, K., Su, H., Dou, Y., 2021. Beyond AP: a new evaluation index for multiclass classification task accuracy. Appl. Intell. 51, 7166–7176. https://doi.org/10.1007/s10489-021-02223-7.